Modelling of Rotor-gas bearings for Feedback Controller Design

Theisen, Lukas Roy Svane; Niemann, Hans Henrik

Published in:
Journal of Physics: Conference Series (Online)

Link to article, DOI:
1088/1742-6596/570/5/052005

Publication date:
2014

Modelling of Rotor-gas bearings for Feedback Controller Design

Lukas R. S. Theisen, Henrik Niemann

Department of Electrical Engineering, Technical Unversity of Denmark, Elektrovej, Bld. 326, 2800 Kgs. Lyngby, Denmark

E-mail: lrst@elektro.dtu.dk

Abstract. Controllable rotor-gas bearings are popular offering adaptability, high speed operation, low friction and clean operation. Rotor-gas bearings are however highly sensitive to disturbances due to the low friction of the injected gas. These undesirable damping properties call for controllers, which can be designed from suitable models describing the relation from actuator input to measured shaft position. Current state of the art models of controllable gas bearings however do not provide such relation, which calls for alternative strategies. The present contribution discusses the challenges for feedback controller design using the state of the art method, and an alternative data driven modelling approach is pursued based on Grey-Box system identification. The method allows development of models of the rotor-gas bearing suitable for controller design, which can be identified from data over the range of operation and are shown to accurately describe the dynamical behaviour of the rotor-gas bearing. Design of a controller using the identified models is treated and experiments verify the improvement of the damping properties of the rotor-gas bearing.

1. Introduction

Controllable gas bearings are popular for offering high speed operation at low friction using clean and abundant air as a lubricant. Design of such rotor-gas bearing systems has been the topic of a previous PhD project [3] from the Mechanical Engineering department at the Technical University of Denmark (DTU). A result of the work is a piezo actuated rotor-gas bearing test rig. A controller is however required to improve the poor damping properties, and a collaborative PhD has begun between the department of Mechanical Engineering and the Electrical Engineering control engineering group to further explore the design of such controllers. This paper provides an overview of the work so far of the collaborative PhD.

State of the art models of rotor-gas bearings [5, 4] rely on solving the Reynolds equation to model the pressure distribution of the fluid film. Morosi [4] included the effect of the piezo actuated valves into the Reynolds equation, and used it to develop a model of a short rigid rotor-gas bearing actuated by piezo valves based on this modified Reynolds equation (MRE). This model was used to manually tune the parameters of a decentralised controller. Recent work in print has however shown that alternative models of the flow in the valves are required to make the model reflect reality. The MRE requires iteratively solving causing an unknown analytical relation from input to the valves to displacement of the rotating shaft, which leaves the model unsuitable for design of model based controllers. This PhD project has therefore investigated development of such suitable models using system identification, e.g. in [8], which

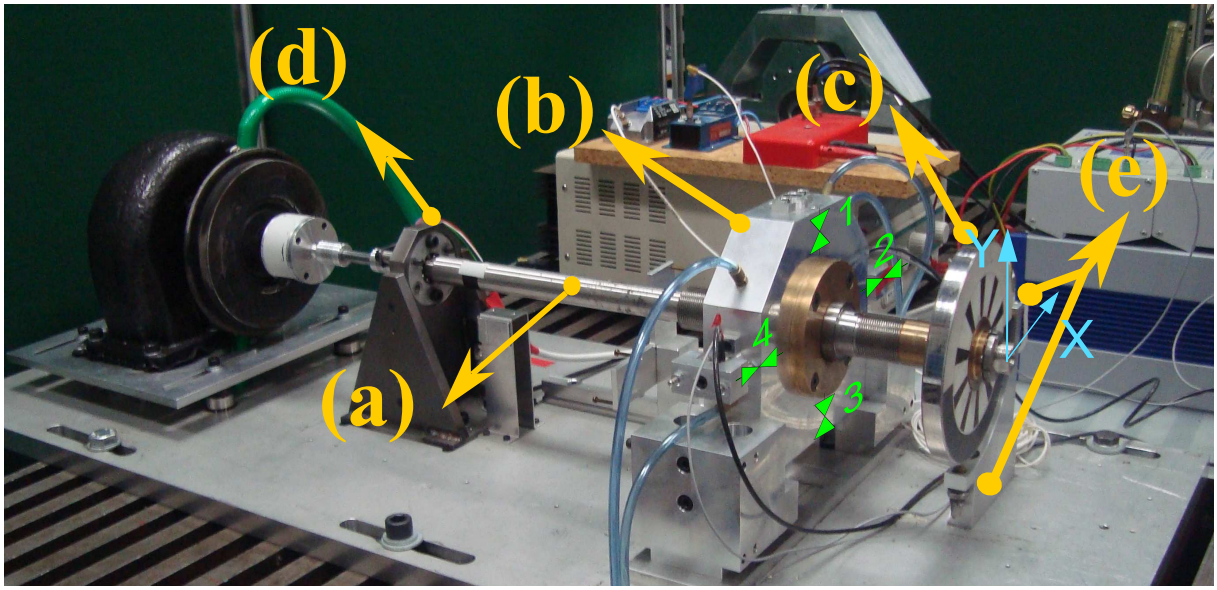

Figure 1. The experimental bearing setup. A flexible shaft (a) is supported by both a ball bearing (d) and the controllable gas bearing (b) with four piezo actuated valves. A disc (c) is mounted in one end to pre-load the journal and displacement sensors (e) measure the lateral movement of the disc.

showed that linear models identified from experimental data could describe the gas bearing behaviour. Models were identified over a range of rotational velocities, where the parameters were found using Grey-Box system identification. The present contribution makes use of the same bearing model and extends the results by also modelling the actuator dynamics.

The present contribution provides an overview of the progress in developing models and their usage for feedback controller design of the rotor-gas bearing from experimental data over the desired operational range determined by rotational velocity and injection pressure. The paper is structured as follows: A brief overview of the experimental test rig is given in Sec. 2, followed by an overview of the current state of the art model and its challenges. Section 4 shows formulation of the Grey-box model and its parameters are identified from experiments. The identified model is used in Sec. 5 to design a controller capable of increasing the damping properties of the rotor-gas bearing and experiments in Sec. 6 verify the capabilities of the designed controller.

2. Experimental Setup of Rotor-Gas Bearing

The experimental setup at hand is shown in Fig. 1: a turbine driven flexible shaft (a) is supported by both a ball bearing (d) and the controllable gas bearing (b), in which pressurised air is injected through four piezo actuated valves numbered as shown. The manometric injection pressure P_I of the pressurised air is measured by a mechanical gauge before splitting up to the four actuators. The absolute pressure in the valves P_{abs} is assumed to be the sum of the measured pressure P_I and the atmospheric pressure P_{atm}. A disc (c) is mounted in one end to pre-load the journal. The horizontal and vertical shaft deflections (e_x, e_y) are measured at the disc location using eddy current sensors (e) in the coordinate frame specified in the figure. The angular position of the shaft ϕ is measured by an optical encoder. The pressurised air generates a thin layer of fluid film in the $25\mu m$ thin gap between the shaft and the bearing housing. For a range of conditions, the fluid film generates restoring forces and thereby keeps the shaft levitating in a stable equilibrium. A more thorough description of the setup is available in [6].

The piezo-electric valves are subject to hysteresis and creep effect [1]. To counteract

the hysteresis, decentralised PD-controllers are deployed, effectively reducing the position uncertainty by counteracting the hysteresis. The controlled valves are commanded reference positions $r_{p,i} \in [0; 10]V$, and the corresponding valve positions $y_{p,i} \in [0; 10]V$ are measured ranging from open valve ($0V$) to closed valve ($10V$). The valves are controlled pairwise as if there was just a single horizontal and a vertical valve commanded position reference $r(t) \triangleq [r_x(t), r_y(t)]^{\mathrm{T}}$, which is mapped as a reference to the individual valves according to the law from $r(t) \to r_p(t)$, similarly the lumped valve position vector $u(t)$ is defined as a function of the individual valve positions:

$$r_p(r_x(t), r_y(t)) = \begin{bmatrix} r_{p,1}(t) \\ r_{p,2}(t) \\ r_{p,3}(t) \\ r_{p,4}(t) \end{bmatrix} = \begin{bmatrix} r_0 + r_y(t) \\ r_0 + r_x(t) \\ r_0 - r_y(t) \\ r_0 - r_x(t) \end{bmatrix}, \qquad u(t) \triangleq \begin{bmatrix} u_x(t) \\ u_y(t) \end{bmatrix} = \begin{bmatrix} y_{p,2}(t) - y_{p,4}(t) \\ y_{p,1}(t) - y_{p,3}(t) \end{bmatrix} \quad (1)$$

This makes the valves cooperate and reduces the system from an over-actuated to a fully actuated. In addition the constant offset $r_0 = 5V$ ensures the largest dynamical range.

3. Rotor-gas Bearing Modelling Using Finite Element Models and the Modified Reynolds Equation

Current state of the art models of the rotor-gas bearing [5, 4] consist of two sub-models: A Finite Element model of the flexible shaft and a model of the thin layer of fluid film. This section provides an overview of these two models and their challenges.

3.1. The Modified Reynolds Equation

The Modified Reynolds equation [4] is used for modelling the behaviour of the thin layer of fluid film in the rotor-gas bearing. By a set of assumptions, a partial differential equation can be made, modelling the pressure p as a function of the fluid film thickness h, which varies along with the shaft position in the bearing and time t can then be set up:

$$\frac{\partial}{\partial \mathsf{y}}\left(\mathsf{ph}^3 \frac{\partial \mathsf{p}}{\partial \mathsf{y}}\right) + \frac{\partial}{\partial \mathsf{z}}\left(\mathsf{ph}^3 \frac{\partial \mathsf{p}}{\partial \mathsf{z}}\right) = 6\mu U \frac{\partial(\mathsf{ph})}{\partial \mathsf{y}} + 12\mu \frac{\partial(\mathsf{ph})}{\partial t} + 12\mathsf{p}V_I \quad (2)$$

where the fluid film coordinate frame $(\mathsf{x}, \mathsf{y}, \mathsf{z})$ chosen is: x the radial coordinate directed towards the centre of the shaft, y the circumferential coordinate and z being the axial coordinate. μ is the viscosity of the gas, U is the linear velocity of the rotating shaft at the bearing housing, V_I is the velocity profile of the injected gas assumed to be parabola shaped with a linear pressure drop along the length of the valves; Work in print however shows this does not model the flow well. The flow is assumed laminar, which is reasonable given the small thickness of the fluid film. The MRE has no known analytical solution, but discretisation in a fine grid allows an iterative solution to be found from a good initial solution guess. This provides the pressure profile, which upon integration provides the horizontal and vertical forces from the fluid film acting on the flexible shaft $F_{be} = [F_{X,be},\ F_{Y,be}]^{\mathrm{T}}$.

3.2. Finite Element Modelling of Flexible Shaft

The flexible shaft can then be modelled using a finite element (FE) method, where the shaft is divided into n_e sections, which can bend and rotate relative to each other around the $n_n = n_e + 1$ nodes connecting the sections giving four degrees of freedom (DOFs) per node. Given the geometry of the shaft and its material properties, the stiffness of each section can be approximated, the mass of each section can be calculated and the forces from each section acting on the other sections can then be expressed as a $n_n \cdot 4$ coupled differential equations with the linear and angular displacements from a horizontal and a vertical axis $q_F = [q_1,\ q_2, \ldots, q_{4n_n}]^{\mathrm{T}}$

with corresponding time derivatives $\dot{q}_F$. The model is formulated using the mass matrix M_F, the stiffness matrix K_F, the gyroscopic matrix G_F and the damping matrix D_F:

$$M_F\ddot{q}_F(t) + (D_F - \Omega G_F)\dot{q}_F(t) + K_F q_F(t) = f_F(t), \quad q_F = [q_1,\, q_2, \ldots, q_{4n_n}]^{\mathrm{T}} \tag{3}$$

where in the above $f_F(t)$ is the external forces acting on each node of the FE model from the fluid film, external disturbances etc.. Using the linearised stiffness and damping forces from the MRE bearing model, the FE model predicts the eigenfrequencies within $\pm 5\%$ in the stationary case over a wide range of injection pressures and rotational velocities.
The requirement of this iteratively solved pressure profile for every configuration however leaves the model unable to describe the relation from actuator input voltage to shaft displacement on a form suitable for controller design. The time dependent MRE still remains to be coupled to the FE shaft model and validated experimentally, before the relation from input voltage to shaft displacement can be approximated and put on an analytical form. This shows the need for alternative approaches to develop models for feedback controller design, which do not depend on the solution of the MRE.

4. A System Identification Approach - Data Driven Modelling

The modelling of rotor gas bearings still represents an open challenge. This section shows a heuristics based model approach, where basic knowledge from rotor-dynamics provides the basis for formulation of a model. The model parameters are then identified from experimental data, where the piezo-valves perturb the rotor-gas bearing. The method allows development of accurate models able to describe the rotor-gas bearing dynamics.

The measurement of the valve positions allows dividing the modelling in two: an actuator sub-model to model the valve dynamics from commanded valve reference position to valve position, and a bearing sub-model to model the relation from valve position to shaft deflection. The parameters of the identified models allow formulation of a global model.

4.1. Grey-Box Model of Gas Bearing

In a rotational range around the first two eigenfrequencies, the rotor gas bearing system consisting of the flexible shaft and the gas-bearing can be modelled as a 2 DOF coupled mass-spring damper system. Let $p = [e_x, e_y]^{\mathrm{T}}$ be the position vector consisting of horizontal and vertical shaft displacements, and denote time derivatives $\frac{d}{dt}(\cdot) = \dot{(\cdot)}$. The model then reads

$$\mathcal{M}\ddot{p}(t) + (\mathcal{D} - \Omega\mathcal{G})\dot{p}(t) + \mathcal{K}\, p(t) = \mathcal{B}_p u(t), \quad p = [e_x, e_y]^{\mathrm{T}}, \tag{4}$$

in which Ω is the rotation speed, $\mathcal{M}$ is the diagonal mass matrix, $\mathcal{D}$ is the damping matrix, $\mathcal{G}$ is the antisymmetric gyroscopic matrix, and $\mathcal{K}$ is the stiffness matrix, all with dimension 2×2. The right hand side should include external forces $f(t)$ acting on the rotor-gas bearing, which include: forces from mass unbalance, forces from the piezo valves and forces from external impacts. Section 4.4 shows how the mass unbalance response is filtered out. In [8] it was shown reasonable to assume the actuator force proportional to the valve position with gain $\mathcal{B}_p$, of dimension 2×2 and the model therefore reduces to Eq. 4. The model is reformulated to state space form to ease the Grey-Box modelling. A suitable choice of states is the deflection and velocity of the shaft $x \triangleq [e_x, e_y, \dot{e}_x, \dot{e}_y]^{\mathrm{T}}$. The measurement noise and errors from simplified model are modelled as additive noise $d(t)$ entering both output and states with a disturbance input gain $\mathcal{B}_d$ and the chosen state space formulation of Eq. (4) then reads:

$$\begin{aligned} \dot{x}(t) &= \mathcal{A}x(t) + \mathcal{B}u(t) + \mathcal{B}_d d(t), \quad x(0) = x_0 \\ p(t) &= \mathcal{C}x(t) + d(t) \end{aligned} \tag{5}$$

where the system-, input gain-, and output matrix are

$$\mathcal{A} = \begin{bmatrix} 0 & I \\ -K & -D \end{bmatrix}, \quad \mathcal{B} = \begin{bmatrix} 0 \\ B \end{bmatrix}, \quad \mathcal{B}_d = \begin{bmatrix} 0 \\ B_d \end{bmatrix}, \quad \mathcal{C} = \begin{bmatrix} I & 0 \end{bmatrix}, \tag{6}$$

where $D \triangleq \mathcal{M}^{-1}(\mathcal{D} - \Omega\mathcal{G})$, $K \triangleq \mathcal{M}^{-1}\mathcal{K}$, and $B \triangleq \mathcal{M}^{-1}\mathcal{B}_p$ are the matrices to be identified along with disturbance gain B_d, and initial value x_0, each with four parameters giving 20 unknowns in total. The parameters of (6) are identified by recasting the problem to a model parametrized in $\hat{\theta}_b \triangleq \{\hat{D}, \hat{K}, \hat{B}, \hat{x}_0, \hat{B}_d\}$ as $\mathfrak{M}_b(\theta)_b$. Each matrix $\hat{D}, \hat{K}, \hat{B}, \hat{B}_d$ has four elements denoted by small letters and subscripts xx, xy, yx, yy. The model then reads

$$\mathfrak{M}_b(\theta_b) : \begin{cases} \dot{x}(t) = \mathcal{A}(\theta_b)x(t) + \mathcal{B}(\theta_b)u(t) + \mathcal{B}_d(\theta_b)d(t), \quad x(0) = x_0(\theta_b) \\ p(t) = \mathcal{C}x(t) + d(t) \end{cases} \tag{7}$$

4.2. Grey-Box Model of Lumped Actuators

This section formulates a similar model of the lumped PD-controlled piezo valves. The closed loop horizontal and vertical lumped valve can each be modelled as a second order low-pass filter. The valve dynamics can be seen as transfer functions with two poles $p_{1,j}$, and $p_{2,j}$, where j refers to the horizontal valve x or vertical valve y and gain $\kappa_{a,j}$. Considering only the commanded reference position as input, the dynamics then read:

$$\begin{bmatrix} u_x(s) \\ u_y(s) \end{bmatrix} = \begin{bmatrix} H_{a,x}(s) & 0 \\ 0 & H_{a,y}(s) \end{bmatrix} \begin{bmatrix} r_x(s) \\ r_y(s) \end{bmatrix}, \qquad H_{a,j}(s) = \frac{\kappa_{a,j}}{\left(\frac{1}{p_{1,j}}s + 1\right)\left(\frac{1}{p_{2,j}}s + 1\right)} \tag{8}$$

in which $H_{a,j}(s)$ is the second order filter of the specified form. The model can be formulated in the same structure as Eq. 7, exploiting that cross coupling terms $k_{xy}, k_{yx}, d_{yx}, d_{xy}, b_{yx}, b_{xy}, b_{p,yx}, b_{p,xy}$ are zero. Reformulating this to a Grey-box model and estimating the initial valve states x_a and a similar disturbance gain d_a, the model then reads

$$\mathfrak{M}_a(\theta_a) : \begin{cases} \dot{x}_a(t) = \mathcal{A}(\theta_a)x_a(t) + \mathcal{B}(\theta_a)r(t) + \mathcal{B}_{d,a}(\theta_a)d_a(t), \quad x_a(0) = x_{a0}(\theta_a) \\ u(t) = \mathcal{C}_a x_a(t) + d_a(t) \end{cases} \tag{9}$$

Estimating the gains, poles, initial state and disturbance gain, the actuator model thus only has 12 parameters being:

$$\theta_a \triangleq [\underbrace{k_{a,xx},\ k_{a,yy},\ b_{a,xx},\ b_{a,yy},\ d_{a,xx},\ d_{a,yy}}_{\text{valve coefficients}},\ \underbrace{b_{da,xx},\ b_{da,yy}}_{\text{disturbance gains}},\ \underbrace{x_{a1,x0},\ x_{a2,x0},\ x_{a3,x0},\ x_{a4,x0}}_{\text{initial state}}]^{\mathrm{T}}, \tag{10}$$

and a similar actuator model $\mathfrak{M}_a(\theta_a)$ has been formulated.

4.3. Description of Experiments

The model should represent the rotor-gas bearing over the range of operational conditions, which are defined by two main characteristics: rotational speed Ω and injection pressure P_I, which can vary within $\Omega \in [0; 6]krpm$ and $P_I \in [3; 7]bar$ respectively. This identification over the whole operational range will be available in [7], where the coefficients are estimated from data sets collected from a grid of injection pressures and rotational velocities representing the range of interest. Here a selected example is chosen $\bar{\Omega} = 0rpm$ and $\bar{P}_I = 4.0bar$. During data collection all variables were sampled at f_s=5kHz. A pseudo random binary sequence commanded as reference for the lumped valves $r(t)$ ensured excitation of the system and hence identifiability of the parameters. The input stepped from -1 to 1 at random sampling instants. The lumped valve references $r(t)$ and measured lumped valve positions $u(t)$ were logged as input and output for the actuator sub-model and the lumped valve positions $u(t)$ and the shaft displacement $p(t)$ as input and outputs for the bearing model.

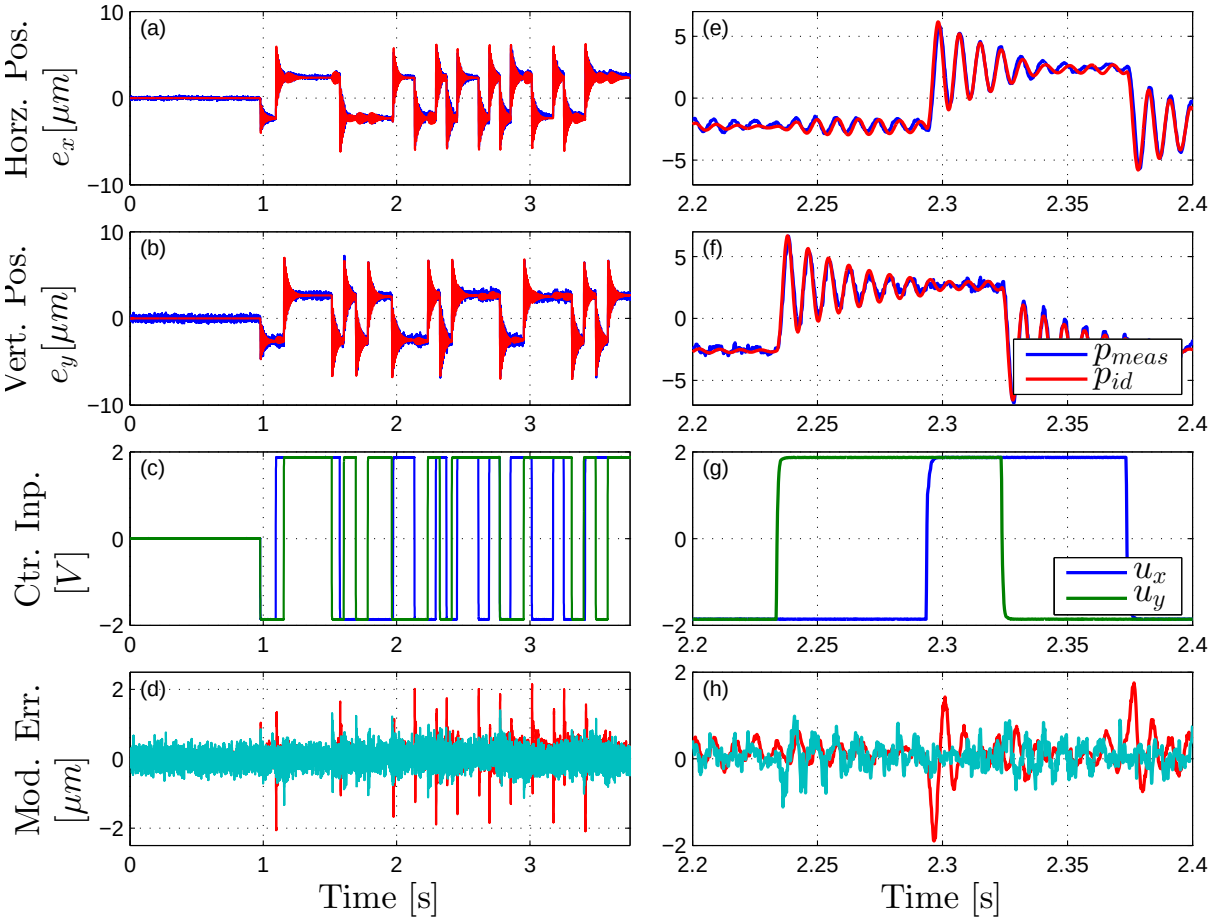

Figure 2. Example of an identification of data set collected at $P_I = 4bar, \Omega = 0rpm$. The valve positions $[u_x, u_y]$ exciting the bearing shown in c) excite the bearing dynamics causing deflection of the shaft. a) and b) show this measured deflection $p_{meas} = [e_x, e_y]$ and the predicted using the identified model $p_{id} = [\hat{e}_x, \hat{e}_y]$ subject to valve excitation. d) shows the residual between identified and measured response $\varepsilon = p_{meas} - p_{id}$. Subplots e, f, g and h show corresponding time zooms.

4.4. Prefiltering

Before identification, the data sets are prefiltered using a run-out filter $\mathcal{F}_r$, which filters out the response from surface unsmoothness and mass unbalance response. This is calculated from a data set collected at each operational condition, where the shaft is not excited, which allows generation of the response as function of encoder angle $\mathcal{F}_r(\phi)$. The offset of both inputs and outputs estimated as mean of the first 2000 samples are subtracted from the data sets. A median filter of size 3 is used to smooth out noise from the shaft position measurements.

4.5. Identification

The parameters of both the actuator sub-model and the bearing sub-model are identified using the prediction error method [2], and initial guesses of the parameters are obtained from previous identified models. The model update iterations were stopped when the relative improvement norm was less than 10^{-4} indicating convergence.

Both the actuator model $\mathfrak{M}_a$ and the bearing model $\mathfrak{M}_b$ are then identified from the respective

data sets. The actuator sub-models are found to be fairly constant over the investigated range of interest, and a nominal actuator model G_{act} is chosen. The bearing model parameters however vary with both injection pressure and rotational velocity as expected from [3]. The model residuals are expected to be white noise, which is not the case as shown in Fig. 2 (d) and (h). The norm of the residual however is small indicating low importance of the residual dynamics.

Cascading of the bearing model and the actuator model provides the total rotor-gas bearing model: $G_p(s) = G_{bear}(s)G_{act}(s)$.

5. H_∞ Control

A suitable control strategy such as the mixed sensitivity-approach can improve the poor damping characteristics of the rotor-gas bearing. The identified model is used for design of such a controller.

The H_∞ controller $K_\infty(s)$ has been designed using the stacked requirements $||N||_\infty = \max_\omega \bar{\sigma}(N(j\omega)) < 1;$, where $N = [W_pS, W_uK_\infty S]^{\mathrm{T}}$. The controller is designed for a model identified at $P_I = 7bar, \Omega = 4000rpm$. The chosen weights W_p and W_u shown in Fig. 3 ensure an increase in damping without counteracting low frequency disturbances such as changes in equilibrium position due to changing operational condition. The controller obtained using the specified weights is reduced from 24 states to a fourth order controller $K_\infty(s)$ using Gramian-based input/output balancing. The reduction factor in sensitivity towards disturbances is determined from the output sensitivity calculated as:

$$S_o(s) \triangleq (\mathbb{I}_2 + G_p(s)K_\infty(s))^{-1} \tag{11}$$

The reassembled bearing model [7] is used to assess performance of the controller over the range of operation. This model is developed from identified models from data collected over a range of injection pressures ($P_I \in [3; 7]bar$) and rotational speeds ($\Omega \in [0; 6]krpm$) and describes the rotor-gas bearing behaviour over the wide range of operational conditions. Figure 4 shows the output sensitivity of the closed loop system for different randomly chosen operational points models within the operational range. The sensitivity is reduced in the desired frequency range from $[70 : 190]Hz$ by a factor three to nine, though at the cost of an increased sensitivity of a factor 1.2 at low frequencies, and a peak sensitivity around $280Hz$ of a factor 1.8, which is affordable.

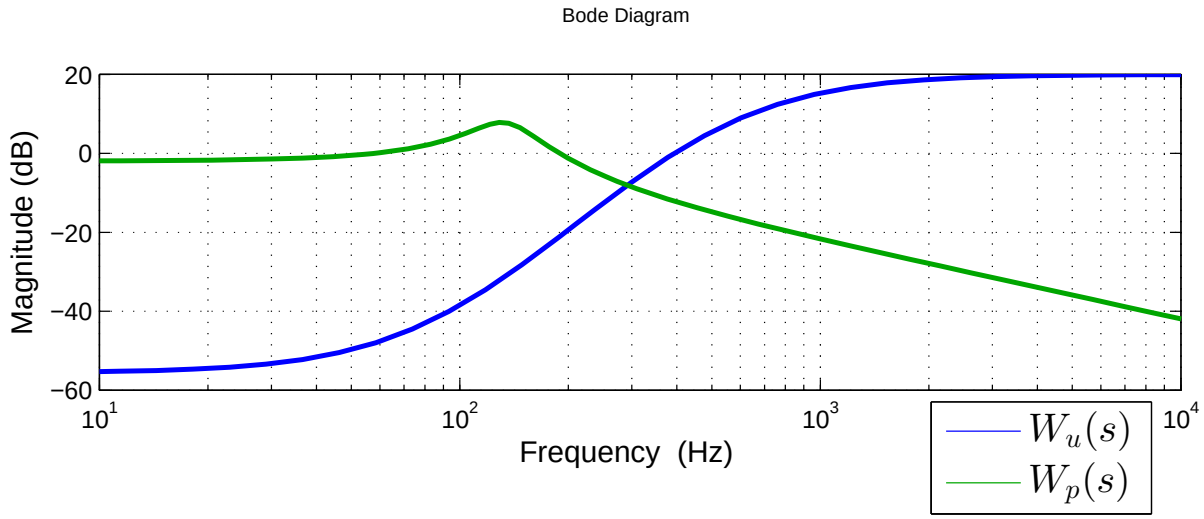

Figure 3. Weights $W_p(s)$ and $W_u(s)$ for mixed sensitivity controller design

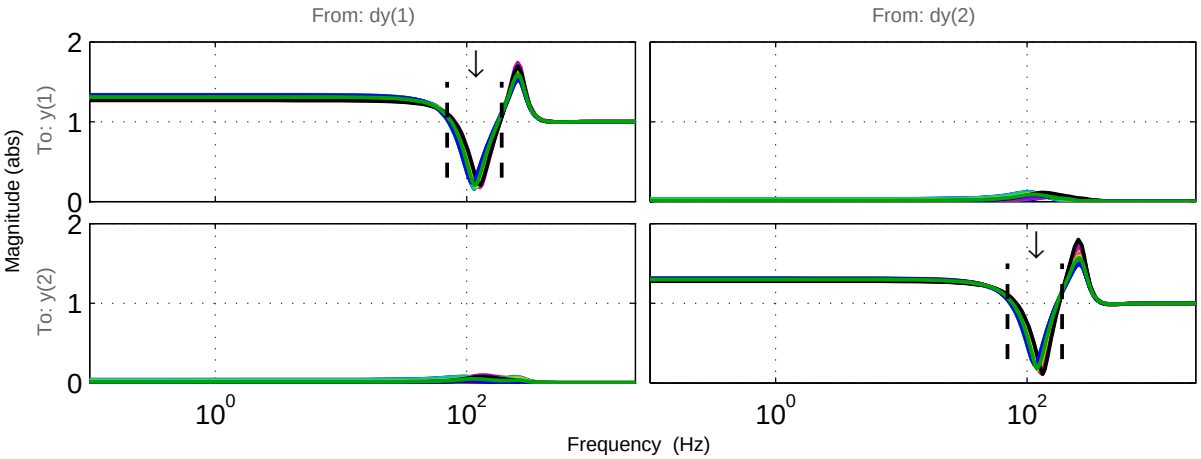

Figure 4. Output sensitivity $S_o(s)$ for $N_r = 30$ realizations of the rotor-gas bearing within the operational. The black arrow and lines mark the frequency interval where the sensitivity is reduced.

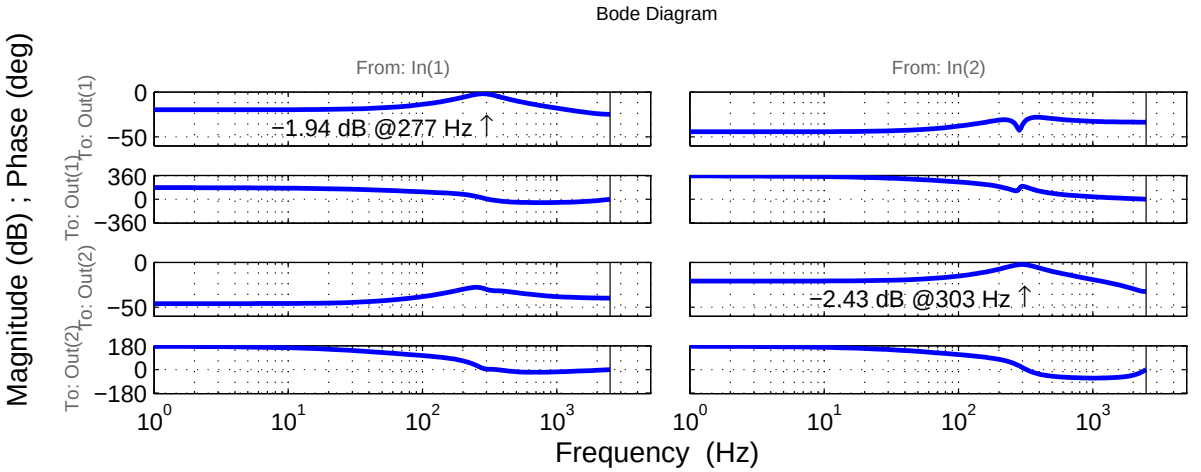

Figure 5. Frequency response of controller $K(z)$

Discretisation of the controller to $K_\infty(z)$ using a Tustin-approximation allows implementation on the rotor-gas bearing test-rig, and the frequency response in Fig. 5 shows the desirable capabilities of the controller: at low frequencies and DC the controller is not active, only in an interval around the critical frequencies is the controller active.

6. Experimental Results

The controller is implemented on the rotor-gas bearing system, and impacts are applied to the rotor-gas bearing both with the controller on and off. Figure 6 shows a horizontal impact response at $\bar{P}_I = 4bar$, $\bar{\Omega} = 0rpm$: using the robust controller, the horizontal damping is found increased from 0.0567 to 0.173 - a factor three. A vertical impact in Fig. 7 shows similar increase in damping. Horizontal and vertical impacts at higher pressure $\bar{P}_I = 7bar$ show a damping increase by a factor six from 0.0282 to 0.1668, which is within the expected range of damping increase predicted by the sensitivity function. Equivalent results can be obtained for non zero rotational velocities.

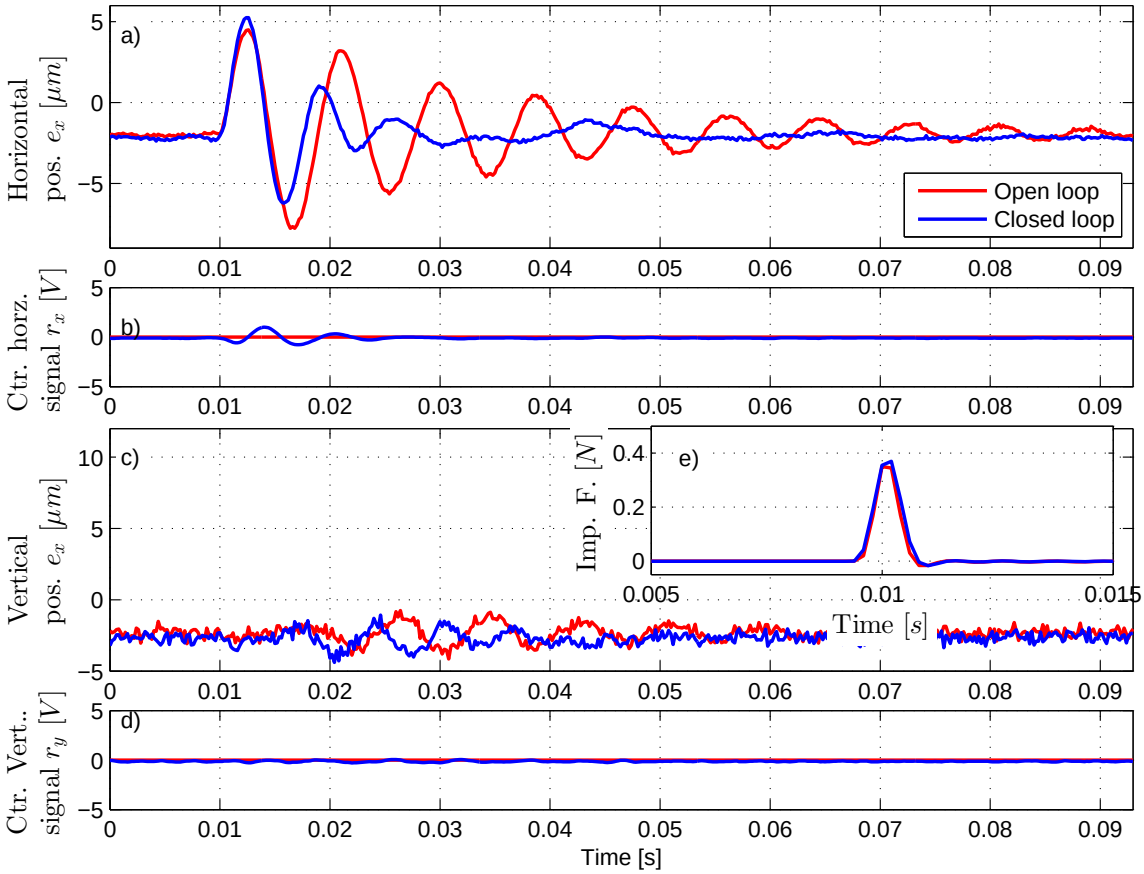

Figure 6. Horizontal impact response without and with the designed controller at $\bar{P}_I = 4bar$, $\bar{\Omega} = 0rpm$. Impact occurs close to time $t = 0.01s$. a and c show measured deflections, b and d show commanded valve positions and e shows the measured impact force.

7. Conclusion

Two Grey-box models were developed modelling the actuators and bearing dynamics for a rotor-gas bearing, and successfully used to identify model parameters describing the relation from commanded to measured valve position, and from valve position to shaft displacement of the rotor-gas bearing. A mixed sensitivity controller was designed to stabilise the rotor-gas, and its increase in damping was validated experimentally for chosen conditions.

Acknowledgments

The Danish Ministry of Science, Innovation and Higher Education is gratefully acknowledged for the support to the FTP research project 12-127502.

References

[1] K. K. Leang and S. Devasia. Iterative feedforward compensation of hysteresis in piezo positioners. *42nd IEEE Conference on Decision and Control, vols 1-6, Proceedings*, pages 2626–2631, 2003.

[2] L. Ljung. *System identification - Theory for the User*. Prentice-Hall, 1999.

[3] S. Morosi. *From Hybrid to Actively-Controlled Gas Lubricated Bearings Theory and Experiment*. PhD thesis, Technical University of Denmark, april 2013.

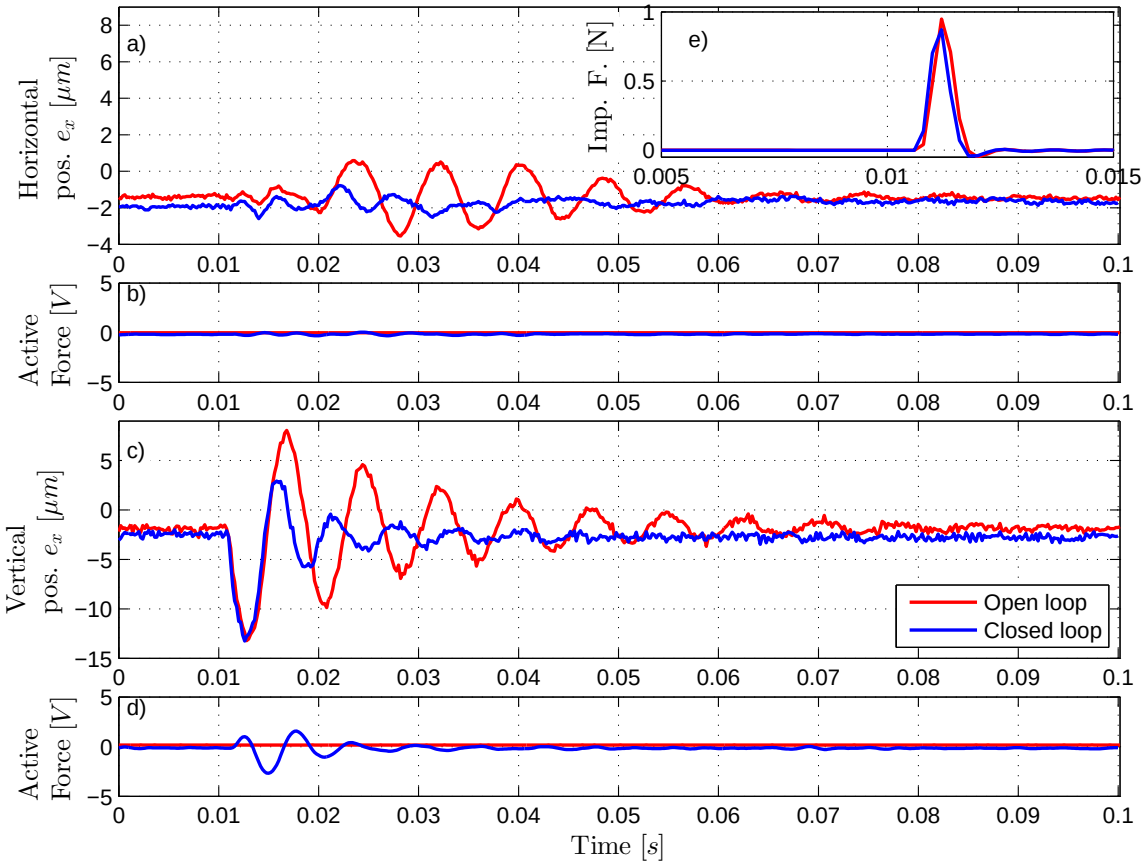

Figure 7. Vertical impact response without and with the designed controller at $\bar{P}_I = 4bar$, $\bar{\Omega} = 0rpm$. Impact occurs close to time $t = 0.01s$. a and c show measured deflections, b and d show commanded valve positions and e shows the measured impact force.

[4] S. Morosi and I. F. Santos. Active lubrication applied to radial gas journal bearings. Part 1: Modeling. *Tribology International*, 44(12):1949–1958, November 2011.

[5] S. Morosi and I. F. Santos. On the modelling of hybrid aerostatic-gas journal bearings. *Proceedings of the Institution of Mechanical Engineers, Part J: Journal of Engineering Tribology*, 225(7):641–653, June 2011.

[6] S. Morosi and I. F. Santos. Experimental investigations of active air bearings. In *ASME Turbo Expo 2012: Turbine Technical Conference and Exposition*. American Society of Mechanical Engineers, 2012.

[7] L. R. S. Theisen, H. Niemann, I. F. Santos, M. Blanke, and R. Galeazzi. Modelling and identification for control of rotor gas bearings. *Submitted to Mechanical Systems and Signal Processing*, 2014.

[8] L. R. S. Theisen, F. G. Pierart Vásquez, H. H. Niemann, I. F. Santos, and M. Blanke. Experimental grey box model identification of an active gas bearing. *Vibration Engineering and Technology of Machinery*, pages 963–976, 2014.